Inorg. Chem. **2008**, *47*, 4977−4987

Studies of the Carbon Dioxide and Epoxide Coupling Reaction in the Presence of Fluorinated Manganese(III) Acacen Complexes: Kinetics of Epoxide Ring-Opening

Donald J. Darensbourg* and Eric B. Frantz

Department of Chemistry, Texas A&M University, College Station, Texas 77843

Received February 13, 2008

Five-coordinate manganese(III) complexes of *N,N′-bis*(trifluoroacetylacetone)-1,2-ethylenediimine (tfacacen) have been synthesized and structurally characterized by X-ray crystallography. The presence of the electron-withdrawing $-CF_3$ substituents enhances the electrophilicity of the metal center in these (tfacacen)MnX (X = Cl, N_3, NCO, NCS) derivatives when compared with their (acacen)MnX (acacen = *N,N′*-bis(acetylacetone)-1,2-ethylenediimine) analogs. This is demonstrated by the increased propensity of the Mn(III) center in the tfacacen complexes to bind a sixth ligand. Binding studies were performed utilizing the υ_{N_3} stretching frequency in (tfacacen)MnN_3, which is sensitive to the coordination of a ligand at the vacant axial site. Of importance, cyclohexene oxide was shown to readily bind to (tfacacen)MnN_3, thereby providing an opportunity for directly monitoring the dependence of the epoxide ring-opening process on the metal complex concentration. In this instance, as has been amply demonstrated in the (salen)CrX case, the ring opening of cyclohexene oxide was found to be second-order in [(tfacacen)MnN_3], with an activation energy of 71.0 ± 6.0 kJ/mol. In the presence of strongly coordinating anions or amine bases, the rate of epoxide ring opening by (tfacacen)MnN_3 was greatly retarded. The manganese cyanate and thiocyanate complexes were examined in an effort to develop other initiators for epoxide ring opening which provide readily accessible infrared spectroscopic probes. Indeed, the thiocyanate ligand was found to be well-suited for monitoring the epoxide ring-opening reaction by infrared spectroscopy.

Introduction

The production of polycarbonates from the coupling of carbon dioxide and epoxides has emerged as a major area of interest to both academic and industrial researchers over the past decade. This is due to the potential for the utilization of CO_2 for the synthesis of these highly valuable polymeric materials from an inexpensive, renewable, and safe-to-handle starting material.[1] Equation 1 depicts the reactions which generally occur during the coupling of CO_2 and a generic epoxide in the presence of a metal catalyst. As indicated in eq 1, this process is often accompanied by the generation of a small amount of consecutive epoxide coupling, resulting in ether linkages randomly dispersed in the polycarbonate chain. Additionally, a more pervasive side product resulting from a back-biting mechanism is cyclic carbonate. This latter occurrence can be a major reaction pathway for processes utilizing aliphatic epoxides such as ethylene, propylene, or styrene oxides.

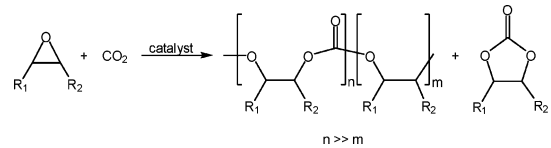

(1)

A wide variety of metal catalysts, including heterogeneous,[2] homogeneous,[3] and supported,[4] have been employed successfully for this process, with Zn(II), Cr(III), and Co(III) metal-based systems having received the most attention. Cyclohexene oxide and propylene oxide are the most widely utilized monomers to date, although various

* Author to whom correspondence should be addressed. Fax (979) 845-0158. E-mail: djdarens@mail.chem.tamu.edu.

(1) (a) Arakawa, H.; Aresta, M.; Armor, J. N.; Barteau, M. A.; Beckman, E. J.; Bell, A. T.; Bercaw, J. E.; Creutz, C.; Dinjus, E.; Dixon, D. A.; Domen, K.; DuBois, D. L.; Eckert, J.; Fujita, E.; Gibson, D. H.; Goddard, W. A.; Goodman, D. W.; Keller, J.; Kubas, G. J.; Kung, H. H.; Lyons, J. E.; Manzer, L. E.; Marks, T. J.; Morokuma, K.; Nicholas, K. N.; Periana, R.; Que, L.; Rostrup-Nielson, J.; Sachtler, W. M. H.; Schmidt, L. D.; Sen, A.; Somorjai, G. A.; Stair, P. C.; Stults, B. R.; Tumas, W. *Chem. Rev.* **2001**, *101*, 953–996. (b) Song, C. *Catal. Today* **2006**, *115*, 2–32. (c) Aresta, M.; Dibenedetto, A. *Dalton Trans.* **2007**, 2975–2992.

10.1021/ic800286p CCC: $40.75
Published on Web 04/26/2008

other epoxides have also been investigated. The first effective homogeneous zinc catalysts reported employed bulky phenoxide or β-diiminate ligands in order to access mono- or dinuclear metal complexes.[5] Other ligands receiving significant attention consist of porphyrins, which have been associated primarily with Cr(III) and Co(III) metal centers.[6] In general, these metal derivatives suffer from being rather expensive and of limited solubility in epoxides. We have recently reported Cr(III) derivatives of an alternative N_4 dianionic ligand system, tetramethyltetraazaannulene, which exhibit real promise as very effective catalysts for CO_2/epoxide coupling reactions.[7] However, the most comprehensively studied metal catalysts are derived from salen(salicylideneimine group) complexes of Cr(III) and Co(III). These latter catalytic systems are binary in nature, in general requiring a cocatalyst or initiator. Common cocatalysts or initiators include Lewis bases such as *N*-heterocyclic amines (e.g., *N*,*N*-dimethylaminopyridine, DMAP) or phosphines, or quaternary organic salts such as PPN^+(bis(triphenylphosphoranylidene)ammonium) or n-Bu_4N^+ salts of chloride, bromide, azide, or pentafluorobenzoate. For the most part, the Cr(III) salen derivatives operate at temperatures between 50−100 °C, whereas the Co(III) salen complexes are active at lower temperatures (25−50 °C). As a consequence of the Co(III) catalysts possessing greater activity at ambient temperature, regio- and stereoregular copolymers are often afforded from the copolymerization process.

Innovations in the area of ligand design continue to appear in the literature. For example, modifications of the salen ligand to incorporate piperidinium end-capping arms or ammonium salts on the phenolate rings of the ligand have led to greatly enhanced activity and selectivity of cobalt(III) catalysts for copolymer versus cyclic carbonate production from propylene oxide and CO_2.[8,9] Varying the transition metal center is another approach to new catalyst development. For example, iron salen complexes have been evaluated as catalysts for the copolymerization of cyclohexene oxide and carbon dioxide and were found to be inactive.[10] A more successful approach was the synthesis of poly(cyclohexylene carbonate) and poly(cyclohexylene oxide) catalyzed by manganese(III) acetate complexes of tetraphenylporphyrin and salen, respectively.[11] We have recently investigated the use of manganese(III) acacen (acacen = *N*,*N*′-bis(acetylacetone)-1,2-ethylenediimine) complexes as catalyst for the copolymerization of cyclohexene oxide and CO_2, and although they were found to be inactive with and without the application of a cocatalyst, they have proven to be useful model complexes for the mechanistic study of the copolymerization process.[12] The inability of the metal center to readily bind essential ligands such as epoxides or apical anions to the open coordination site of the five-coordinate precursor was identified as a key reason for catalytic inactivity. It was concluded that the successful chromium(III) and cobalt(III) salen systems' preference for octahedral geometries is a main contributor to their success.

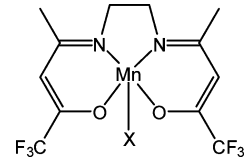

Figure 1. Structures of the (tfacacen)MnX complexes. **1**: X = N_3. **2**: X = Cl. **3**: X = NCO. **4**: X = NCS.

As a consequence of our findings with the (acacen)MnX derivatives, we surmised that an increase in the electrophilicity of the metal center of manganese(III) acacen complexes should facilitate the binding and activation of epoxides. To examine this hypothesis, a series of previously unreported manganese(III) acacen derivatives have been prepared and structurally characterized which possess electron-withdrawing trifluoromethyl groups attached to the carbons α to the coordinated oxygen atoms of the ligand (Figure 1). Included in this investigation is an extensive spectroscopic examination of the binding of various Lewis bases and anions to the metal center of these (tfacacen)MnX complexes, tfacacen = *N*,*N*′-*bis*(trifluoroacetylacetone)-1,2-ethylenediimine. A kinetic study of the epoxide ring-opening process in the presence of these metal complexes is reported.

Experimental Section

Methods and Materials. Unless otherwise stated, all syntheses and manipulations were carried out on a double-manifold Schlenk vacuum line under an argon atmosphere or in an argon-filled glovebox. Methanol, diethyl ether, dichloromethane, and pentane were freshly purified by an MBraun Manual Solvent Purification System packed with Alcoa F200 activated alumina desiccant. Ethanol was freshly distilled from Mg/I_2. Cyclohexene oxide was purchased from TCI America and freshly distilled from CaH_2. Ethylenediamine (Aldrich), sodium azide (Aldrich), sodium cyanate

(2) (a) Inoue, S.; Koinuma, H.; Tsuruta, T. *J. Polym. Sci., Part B: Polym. Lett.* **1969**, *7*, 287–292. (b) Kuran, W.; Pasykiewicz, S.; Skupinska, J.; Rokicki, A. *Makromol. Chem.* **1976**, *177*, 11–20. (c) Kobayashi, M.; Inoue, S.; Tsuruta, T. *J. Polym. Sci., Polym. Chem. Ed.* **1973**, *11*, 2383–2385. (d) Soga, K.; Imai, E.; Hattori, I. *Polym. J.* **1981**, *13*, 407–410. (e) Motika, S. Air Products and Chemicals, Inc., Acro Chemical Co., and Mitsui Petrochemical Industries Ltd.; U.S. Patent 5,026,676, 1991. (f) Gorecki, P.; Kuran, W. *J. Polym. Sci., Part C: Polym. Lett.* **1985**, *23*, 299–304. (g) Ree, M.; Bae, J. Y.; Jung, J. H.; Shin, T. J. *J. Polym. Sci., Part A: Polym. Chem.* **1999**, *37*, 1863–1876. (h) Rokicki, A.; Kuran, W. *J. Macromol. Sci., Rev. Macromol. Chem.* **1981**, *C21*, 135–186.

(3) (a) Beckman, E. J. *Science* **1999**, *283*, 946–947. (b) Chisholm, M. H.; Zhou, Z. *J. Mater. Chem.* **2004**, *14*, 3081–3092. (c) Coates, G. W.; Moore, D. R. *Angew. Chem., Int. Ed.* **2004**, *43*, 6618–6639. (d) Sugimoto, H.; Inoue, S. *J. Polym. Sci., Part A: Polym. Chem.* **2004**, *42*, 5561–5573. (e) Darensbourg, D. J. *Chem. Rev.* **2007**, *107*, 2388–2410.

(4) Baleizã, O. C.; Garcia, H. *Chem. Rev.* **2006**, *106*, 3987–4043.

(5) (a) Darensbourg, D. J.; Holtcamp, M. W. *Macromolecules* **1995**, *28*, 7577–7579. (b) Cheng, M.; Lobkovsky, E. B.; Coates, G. W. *J. Am. Chem. Soc.* **1998**, *120*, 11018–11019.

(6) (a) Kruper, W. J.; Dellar, D. W. *J. Org. Chem.* **1995**, *60*, 725–727. (b) Mang, S.; Cooper, A. I.; Colclough, M. E.; Chauhan, N.; Holmes, A. B. *Macromolecules* **2000**, *33*, 303–308. (c) Sugimoto, H.; Kuroda, K. *Macromolecules* **2008**, *41*, 312–317.

(7) Darensbourg, D. J.; Fitch, S. B. *Inorg. Chem.* **2007**, *46*, 5474–5476.

(8) Nakano, K.; Kamada, T.; Nozaki, K. *Angew. Chem., Int. Ed.* **2006**, *45*, 7274–7277.

(9) Noh, E. K.; Na, S. J.; Kim, S.-W.; Lee, B. Y. *J. Am. Chem. Soc.* **2007**, *129*, 8082–8083.

(10) Darensbourg, D. J.; Ortiz, C. G.; Billodeaux, D. R. *Inorg. Chim. Acta* **2003**, *357*, 2143–2149.

(11) Sugimoto, H.; Ohshima, H.; Inoue, S. *J. Polym. Sci., Part A: Polym. Chem.* **2003**, *41*, 3549–3555.

(12) Darensbourg, D. J.; Frantz, E. B. *Inorg. Chem.* **2007**, *46*, 5967–5978.

(Alfa Aesar), potassium thiocycante (MCB), tetra-*n*-butylammoniumazide (TCI America), and $Mn(OAc)_3 \cdot 2H_2O$ (Strem Chemicals Inc.) were all used as received without further purification. DMAP (Aldrich) was recrystallized from ethanol/diethyl ether. 1,1,1-Trifluoro-2,4-pentanedione (Aldrich Organics) was dried over molecular sieves before use. Bone-dry carbon dioxide equipped with a liquid dip tube was purchased from Scott Specialty Gases.

The synthesis of *N*,*N*′-bis(trifluoroacetylacetone)-1,2-ethylenediimine [(tfacacen)H_2] was adapted from a literature procedure.[13] Elemental analysis was provided by Canadian Microanalytical Service LTD, Delta, British Columbia. All infrared spectra were recorded using a Mattson 6021 FTIR spectrometer with DTGS and MCT detectors. All ^{1}H NMR were acquired using Unity+ 300 MHz and VXR 300 MHz superconducting NMR spectrometers.

Synthesis of *N*,*N*′-Bis(trifluoroacetylacetone)-1,2-ethylenediimine [(tfacacen)H_2]. An ethanol solution was prepared by the addition of 5.00 g (32.4 mmol) of 1,1,1-trifluoro-2,4-pentanedione to 40 mL of freshly distilled EtOH in a 100-mL round-bottom flask equipped with a stir bar. This flask was placed in an ice bath (0 °C), and to it was added dropwise 0.975 g (16.2 mmol) of ethylenediamine. The resulting mixture was stirred for 4 h while being warmed to room temperature. The flask was then placed in a freezer for 18 h. The final product was collected by filtration, rinsed with cold ethanol, and air-dried. Yield: 1.62 g (30.2%) of colorless crystals. ^{1}H NMR ($CDCl_3$, 300 MHz): δ 11.20 (s, 2H), 5.39 (s, 2H), 3.63 (t, 4H), 2.07 (s, 6H). Anal. calcd for $C_{12}H_{14}F_6N_2O_2$: C, 43.38; H, 4.25; N, 8.43. Found: C, 43.60; H, 4.26; N, 8.64.

Synthesis of [*N*,*N*′-Bis(trifluoroacetylacetone)-1,2-ethylenediimine] Manganese(III) Azide [(tfacacen)MnN_3] (1). To a 250-mL round-bottom flask were added 1.00 g of (tfacacen)H_2 (3.00 mmol) and 0.949 g of $Mn(OAc)_3 \cdot 2H_2O$ (3.54 mmol) along with 40 mL of MeOH and a large stir bar. After 18 h of reaction time, the solvent was removed by rotary evaporation, and the resulting solid was dissolved in 100 mL of water. Unreacted starting material was removed by filtration, and the aqueous solution was added to a 1000-mL separatory funnel. Any residual ligand was extracted with 50 mL of CH_2Cl_2 and discarded. To this solution was added 30 g of NaN_3, and it was dissolved by vigorous shaking, resulting in the formation of a brown precipitate. The product was extracted by 2 × 200 mL portions of CH_2Cl_2 and collected in a 500-mL round-bottom flask equipped with a stir bar. After reducing the solution volume to approximately 300 mL, 10 g of Na_2SO_4 was added, and the mixture was stirred for 1 h. The solution was filtered and reduced to a minimal volume. The final product was recrystallized by the slow addition of 200 mL of diethyl ether followed by filtration to give 1.28 g (61.6% yield) of a dark brown solid. The magnetic moment of complex **1** was determined by Evans' method to be 4.79 μ_B. Anal. calcd for $C_{12}H_{12}F_6N_5O_2Mn$: C, 33.74; H, 2.83; N, 16.39. Found: C, 33.61; H, 2.61; N, 15.77.

Synthesis of [*N*,*N*′-Bis(trifluoroacetylacetone)-1,2-ethylenediimine] Manganese(III) Chloride [(tfacacen)MnCl] (2). The same procedure employed for preparing **1** was used, replacing NaN_3 with NaCl. A dark green microcrystalline product was collected (76.8% yield). Crystals suitable for X-ray analysis were obtained by the slow diffusion of diethyl ether into a CH_2Cl_2 solution of the complex. Anal. calcd for $C_{12}H_{12}F_6ClN_2O_2Mn$: C, 34.27; H, 2.88; N, 6.66. Found: C, 34.15; H, 2.74; N, 6.68.

Synthesis of [*N*,*N*′-Bis(trifluoroacetylacetone)-1,2-ethylenediimine] Manganese(III) Isocyanate [(tfacacen)MnNCO] (3). The same procedure employed for **1** was used, replacing NaN_3 with NaOCN. A dark brown microcrystalline product was collected (42.7% yield). Crystals suitable for X-ray analysis were obtained by the slow diffusion of diethyl ether into a CH_2Cl_2 solution of the complex. Anal. calcd for $C_{13}H_{12}F_6N_3O_3Mn$: C, 36.55; H, 2.83; N, 9.84. Found: C, 36.37; H, 2.73; N, 9.71.

Synthesis of [*N*,*N*′-Bis(trifluoroacetylacetone)-1,2-ethylenediimine] Manganese(III) Isothiocyanate [(tfacacen)MnNCS] (4). The same procedure employed for preparing **1** was used, replacing NaN_3 with KSCN. A green microcrystalline product was collected (78.7% yield). Crystals suitable for X-ray analysis were obtained by the slow diffusion of diethyl ether into a CH_2Cl_2 solution of the complex. Anal. calcd for $C_{13}H_{12}F_6SN_3O_2Mn$: C, 35.23; H, 2.73; N, 9.48. Found: C, 34.33; H, 2.57; N, 9.71.

Statistical Deconvolution of FTIR Spectra. Where noted, FTIR spectra were deconvoluted using Peakfit, version 4.12.[14] Statistical treatment was a residuals method utilizing a combination Gaussian−Lorentzian summation of amplitudes with a linear baseline and Savitsky−Golay smoothing.

Rate Studies. Reactions involving the ring-opening of cyclohexene oxide by **1**, **3**, and **4** were monitored via FTIR by the removal and analysis of solution aliquots at intervals of 5−10 min. The reaction mixtures were heated in an oil bath and stirred under argon. Solution aliquots were collected by a syringe needle and injected into an IR cell. For reaction order studies, four CH_2Cl_2 solutions of 67:1, 100:1, 150:1, and 225:1 CHO/catalyst ratios were analyzed with time at 25 °C. For activation energy determination, four CH_2Cl_2 solutions of CHO/catalyst = 67 were monitored at 10, 20, 25, and 30 °C.

Copolymerization Reactions. Polymerization experiments were performed using a 300-mL Parr autoclave heated to 80 °C overnight under a vacuum. Reaction mixtures were prepared by dissolving 50 mg of the catalyst and an appropriate amount of cocatalyst in neat cyclohexene oxide and then were added to the reactor by injection port. Typical reactions were run at 60−80 °C under 35−55 bar of CO_2 pressure for 6 h. Following each reaction, the contents of the reactor were dissolved in CH_2Cl_2 and analyzed by FTIR to ascertain the presence of cyclic carbonate and polycarbonate. Percent CO_2 linkages was determined by ^{1}H NMR.

X-Ray Structural Studies. Single crystals of **2**, **3**, and **4** suitable for X-ray diffraction were obtained by the slow diffusion of diethyl ether into concentrated CH_2Cl_2 solutions of the respective compound. Single crystals of [(tfacacenMnO)]$_2$ were obtain by the slow evaporation of a reaction mixture containing **1** dissolved in neat cyclohexene oxide. For all reported structures, a Leica IC A, MZ 75 microscope was used to identify suitable crystals of the same habit. Each crystal was coated in paratone oil, affixed to a Nylon loop, and placed under streaming nitrogen (110 K) in a Bruker SMART 1000 CCD or Bruker-D8 Adv GADDS diffractometer. Table 1 contains crystallographic data for the four structures reported herein. Space group determination was made on the basis of systematic absences and intensity statistics. Crystal structures were solved by direct methods and refined by full-matrix least-squares on F^2. All H atoms were placed in idealized positions with fixed isotropic displacement parameters equal to 1.5 times (1.2 for methyl protons) the equivalent isotropic displacement parameters

(13) McCarthy, P. J.; Hovey, R. J.; Ueno, K.; Martell, A. E. *J. Am. Chem. Soc.* **1955**, *77*, 5820–5824.

(14) *Peakfit for Windows*, v.4.12; SYSTAT Software Inc: San Jose, CA, 2003.

Table 1. Crystallographic Data for (tfacacen)MnX Derivatives

	2	**3**	**4**	[(tfacacen)MnOH]$_2$
empirical formula	$C_{12}H_{12}ClF_6MnN_2O_2$	$C_{13}H_{12}F_6MnN_3O_3$	$C_{27}H_{26}Cl_2F_{12}Mn_2N_6O_4S_2$	$C_{30}H_{34}F_{12}Mn_2N_4O_7$
fw	420.63	427.20	971.44	900.49
temp (K)	110(2)	110(2)	110(2)	110(2)
cryst syst	monoclinic	monoclinic	monoclinic	monoclinic
space group	$P2_1/n$	$P2_1/c$	Cc	$P2_1/n$
a (Å)	11.314(3)	7.8313(13)	21.596(8)	9.8052(12)
b (Å)	12.587(3)	18.525(3)	11.332(4)	15.8879(19)
c (Å)	11.775(3)	12.565(2)	15.887(6)	12.0655(15)
β (deg)	110.135(5)	118.476(11)	101.996(6)	107.354(2)
V (Å^3)	1574.4(7)	1602.3(5)	3803(2)	1794.1(4)
D(calcd)(g/cm^3)	1.775	1.771	1.697	1.667
Z	4	4	4	2
abs coeff (mm^{-1})	1.081	7.538	1.015	0.817
obsd reflns	3564	2350	8477	3023
unique reflns [$I > 2\sigma(I)$]	2099	1740	7549	2556
restraints/params	0/219	0/237	2/500	0/255
goodness-of-fit on F^2	1.004	0.997	1.005	1.001
R,[a] [$I > 2\sigma(I)$]	0.0547	0.0649	0.0578	0.0535
R_w,[b] [$I > 2\sigma(I)$]	0.1178	0.1631	0.1507	0.1292

[a] $R = \sum||F_o| - |F_c||/\sum|F_o|$. [b] $R_w = \{[\sum w(F_o^2 - F_c^2)^2]/[\sum w(F_o^2)^2]\}^{1/2}$, $w = 1/[\sigma^2(F_o^2) + (aP)^2 + bP$, where $P = [\max(F_o^2),0 + 2(F_c^2)]/3$.

of the atom to which they are attached. All non-hydrogen atoms were refined using anisotropic displacement parameters.

Programs used were as follows: data collection and cell refinement, SMART WNT/2000, version 5.632,[15] or FRAMBO, version 4.1.05 (GADDS);[16] data reductions, SAINTPLUS, version 6.63;[17] absorption correction, SADABS;[18] structural solutions, SHELXS-97;[19] structural refinement, SHELXL-97;[20] graphics and publication materials, SHEXTL, version 6.14,[21] and X-Seed, version 1.5.[22]

Results and Discussion

Synthesis and X-Ray Structures. Straightforward methods for the synthesis of manganese(III) complexes of the general formula (acacen)MnX have been described by Boucher and Day.[23] Their methodology involves the reaction of $Mn(OAc)_3 \cdot 2H_2O$ and H_2acacen to provide (acacen)MnOAc with subsequent metathesis of the acetate derivative with NaX to yield the desired (acacen)MnX complex. The (tfacacen)MnX complexes (**1**−**4**) were prepared in a similar manner via the intermediate (tfacacen)MnOAc and NaX. The presence of the $-CF_3$ substituents on the acacen ligand greatly reduces the solubility of the resulting (tfacacen)MnX complexes. This hampered the utilization of a more convenient route which we previously employed for the synthesis of acacen derivatives which relied on the formation of a reactive nitrate intermediate salt in aqueous solution.[12] Crystallographic data for the X-ray structures of complexes **2**, **3**, and **4** are presented in Table 1, with pertinent bond angles and distances presented in Table 2.

Table 2. Selected Bond Distances and Angles for Complexes **2**, **3**, **4**, and [(tfacacen)MnO]$_2$

		2	
		N_2O_2 Plane	
Mn(1)−O(1)	1.886(3)	Mn(1)−N(1)	1.991(3)
Mn(1)−O(2)	1.901(3)	Mn(1)−N(2)	1.972(3)
Mn(1)−Cl(1)	2.3807(12)	O(1)−Mn(1)−N(1)	91.10(13)
O(2)−Mn(1)−O(1)	88.92(12)	N(1)−Mn(1)−N(2)	83.74(14)
O(2)−Mn(1)−N(2)	91.12(13)		
		3	
		N_2O_2 Plane	
Mn(1)−O(1)	1.911(4)	Mn(1)−N(1)	2.022(5)
Mn(1)−O(2)	1.919(4)	Mn(1)−N(2)	1.981(4)
O(2)−Mn(1)−O(1)	92.40(15)	O(1)−Mn(1)−N(1)	92.06(17)
O(2)−Mn(1)−N(2)	90.80(17)	N(1)−Mn(1)−N(2)	83.07(18)
		Isocyanate Bridge, $\mu_{1,3}$	
Mn(1)−O(3)	2.424(4)	Mn(1)−N(3)	2.137(5)
N(3)−C(13)	1.163(7)	C(13)−O(3)	1.211(7)
O(1)−Mn(1)−N(3)	96.23(17)	Mn(1)−N(3)−C(13)	176.8(5)
O(1)−Mn(1)−O(3)	87.69(15)	Mn(1)−O(3)−C(13)	129.2(4)
		Metal-to-Metal	
Mn−Mn (polymeric)	6.31(6)		
		4	
		N_2O_2 Plane	
Mn(1)−O(1)	1.907(3)	Mn(2)−O(3)	1.907(3)
Mn(1)−O(2)	1.916(3)	Mn(2)−O(4)	1.916(3)
Mn(1)−N(1)	1.999(3)	Mn(2)−N(4)	1.984(4)
Mn(1)−N(2)	1.995(4)	Mn(2)−N(5)	1.963(4)
O(2)−Mn(1)−O(1)	93.09(13)	O(4)−Mn(2)−O(3)	93.44(13)
O(2)−Mn(1)−N(2)	91.11(15)	O(4)−Mn(2)−N(5)	91.30(15)
O(1)−Mn(1)−N(1)	92.38(14)	O(3)−Mn(2)−N(4)	91.65(15)
N(1)−Mn(1)−N(2)	83.08(14)	N(4)−Mn(2)−N(5)	83.04(16)
		Isothiocyanate Bridge, $\mu_{1,3}$	
Mn(1)−N(3)	2.202(4)	Mn(2)−N(6)	2.168(4)
Mn(2)−S(1)	2.9036(15)	Mn(1)−S(2)	2.8367(15)
N(3)−C(13)	1.150(6)	C(13)−S(1)	1.640(5)
N(6)−C(26)	1.166(6)	C(26)−S(2)	1.638(4)
Mn(1)−N(3)−C(13)	173.4(4)	Mn(2)−N(6)−C(26)	162.8(4)
Mn(2)−S(1)−C(13)	96.74(14)	Mn(1)−S(2)−C(26)	107.12(15)
		Metal-to-Metal	
Mn(1)−Mn(1) (poly.)	12.19(4)	Mn(1)−Mn(2)	6.28(2)
		[(tfacacen)MnO]$_2$	
Mn(1)−O(1)	1.9301(19)	Mn(1)−N(1)	2.038(2)
Mn(1)−O(2)	1.970(2)	Mn(1)−N(2)	1.982(2)
Mn(1)−O(3)	1.8103(19)	Mn(1)−Mn(1)#	2.7326(8)
Mn(1)−O(3)#	1.821(2)	O(1)−Mn(1)−N(2)	168.82(9)
Mn(1)−O(3)−Mn(1)	97.63(9)	O(3)−Mn(1)−O(3)#	82.38(9)

(15) *SMART*, v.5.632; Bruker AXS Inc.: Madison, WI.
(16) *FRAMBO:FRAME Buffer Operation*, v.41.05; Bruker AXS Inc.: Madison, WI.
(17) *SAINT*, v.6.63; Bruker AXS Inc.: Madison, WI.
(18) Sheldrick, G. M. *SADABS*; Bruker AXS Inc.: Madison, WI.
(19) Sheldrick, G. *SHELXS-97*; Institüt für Anorganische Chemie der Universität: Gottingen, Germany, 1997.
(20) Sheldrick, G. *SHELXL-97*; Institüt für Anorganische Chemie der Universität: Gottingen, Germany, 1997.
(21) Sheldrick, G. M. *SHELXTL*, v.6.14; Bruker-Nonius Inc.: Madison, WI, 2000.
(22) Barbour, L. J. *J. Supramol. Chem.* **2001**, *1*, 189–191.
(23) Boucher, L. J.; Day, V. W. *Inorg. Chem.* **1977**, *16*, 1360–1367.

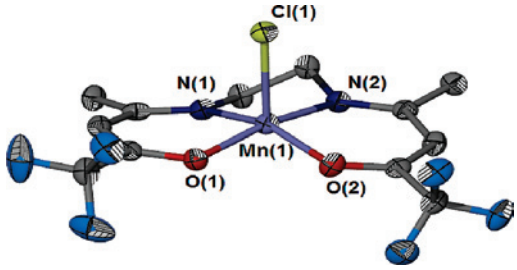

Figure 2. Thermal ellipsoid plot of complex **2** at 50% probability. Hydrogen atoms were omitted for clarity.

Unfortunately, attempts to characterize complex **1** crystallography have thus far failed. However, numerous examples of azide-bridged solid-state extended 1-D polymeric structures exist for similar complexes containing manganese(III) with both acacen and salen derivatives.[24,25] The structure of complex **2** is shown in Figure 2 and, like the nonfluorinated version, is a five-coordinate, near-square-pyramidal complex.[23] In this instance, the structure, however, takes on a step-type ring system where the two planes composed of O(1)−N(1)−C(1)−C(3) (ring 1) and O(2)−N(2)−C(4)−C(6) (ring 2) are 5.9° above and 9.1° below the N_2O_2 plane, respectively (Table 3). Such deviation is likely due to the added steric bulk of the two $-CF_3$ groups. In other respects, the bond angles and distances of the coordination sphere are comparable, including a large metal displacement of 0.311 Å (compared to 0.344 Å for the nonflourinated structure).

The polymeric solid-state structure of complex **3** is presented in Figure 3. As with azide, a helical shape is obtained through bridging cyanates where Mn(1)−O(3) and Mn(1)−N(3) bonds are elongated over the longest ligand nitrogen and oxygen bonds by 0.505 and 0.115 Å, respectively. Though the nature of the $\mu_{1,3}$ bridge complicates the determination of whether the anion is O(3)-bound (cyanate) or N(3)-bound (isocyanate), the greater degree of elongation of the metal−oxygen bond along with evidence to be presented later (vide infra) reliably indicates that the latter case is the one most probable. The helical shape can be attributed to the Mn(1)−O(3)−C(13) bond angle of 129.2(4)° which, combined with a C(13)−O(3) bond length of 1.211(7) Å, indicates sp^2 hybridization at O(3). Steric interactions between adjacent complexes along the coordination chain lead to prominent deformation of the tfacacen ring system where ring 2 lies 25.9° below the N_2O_2 plane and at a dihedral angle of 31.8° to ring 1.

The structure of complex **4** also reveals a helical 1-D coordination polymer comprised of a dimetallic asymmetric unit (Figure 4). Many examples of nitrogen-bound thiocyanate complexes of manganese have been characterized with instances of $\mu_{1,3}$ bridging and bridged polymer chains.[24,26,27] Day et al. solved the polymeric structure of $(acac)_2MnSCN$ with nitrogen and sulfur metal-bond distances of 2.189(5) and 2.880(2) Å, respectively.[28] Complex **4** exhibits similar distances with Mn(1)−N(3) and Mn(2)−N(6) equal to 2.202(4) and 2.168(4) Å along with Mn(1)−S(2) and Mn(2)−S(1) equal to 2.8367(15) and 2.9036(15) Å, respectively. It appears that a trans influence of the sulfur donor ligand exists where a shorter Mn(1)−S(2) bond distance results in an elongated Mn(1)−N(3) distance. The most striking feature of the structure is the pronounced zigzag shape of the thiocyanate−manganese chain, consisting of carbon−sulfur−manganese bond angles of 107.12(15)° and 96.74(14)°. In the latter case, the angle approaches 90°,

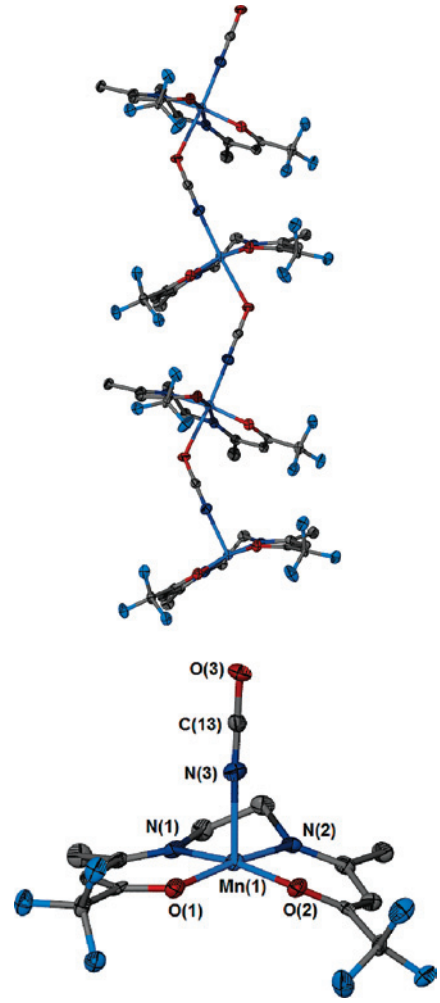

Figure 3. Thermal ellipsoid plot of complex **3** at 50% probability and the polymer chain viewed along the *c* axis. Hydrogen atoms were omitted for clarity.

(24) (a) Panja, A.; Shaikh, N.; Vojtisek, P.; Gao, S.; Banerjee, P. *New J. Chem.* **2002**, *26*, 1025–1028. (b) Saha, S.; Mal, D.; Koner, S.; Bhattacherjee, A.; Gütlich, P.; Mondal, S.; Mukherjee, M.; Okamoto, K.-I. *Polyhedron* **2004**, *23*, 1811–1817. (c) Deoghoria, S.; Bera, S. K.; Moulton, B.; Zaworotko, M. J.; Tuchagues, J. -P.; Mostafa, G.; Lu, T. -H.; Chandra, S. K. *Polyhedron* **2005**, *24*, 343–350. (d) Lu, Z.; Yuan, M.; Pan, F.; Gao, S.; Zhang, D.; Zhu, D. *Inorg. Chem.* **2006**, *45*, 3538–3548. (e) Ko, H. H.; Lim, J. H.; Kim, H. C.; Hong, C. S. *Inorg. Chem.* **2006**, *45*, 847–8849. (f) Miyasaka, H.; Saitoh, A.; Abe, S. *Coord. Chem. Rev.* **2007**, *251*, 2622–2664. (g) Yuan, M.; Zhao, F.; Zhang, W.; Wang, Z.-M.; Gao, S. *Inorg. Chem.* **2007**, *46*, 11235–11242.

(25) Feng, Y. *Chin. J. Struct. Chem.* **2002**, *21*, 352–354.

(26) (a) Sakata, K.; Nakamura, H.; Hashimoto, M. *Inorg. Chim. Acta* **1984**, *83*, L67–L70. (b) Massoud, S. S.; Mautner, F. A. *Inorg. Chim. Acta* **2005**, *358*, 3334–3340. (c) Sen, S.; Mitra, S.; Luneau, D.; Fallah, M. S. E.; Ribas, J. *Polyhedron* **2006**, *25*, 2737–2744. (d) Zhou, Y.-X.; Zheng, X.-F.; Han, D.; Zhang, H.-Y.; Shen, X.-Q.; Niu, C.-Y.; Chen, P.-K.; Hou, H.-W.; Zhu, Y. *Synth. React. Inorg. Met. Org. Chem.* **2006**, *36*, 693–699. (e) Bréfuel, N.; Shova, S.; Tuchagues, J.-P. *Eur. J. Chem.* **2007**, 4326–4334.

(27) Feng, Y. L.; Liu, S. X. *J. Coord. Chem.* **1998**, *44*, 81–90.

(28) Stults, B. R.; Day, R. O.; Marianelli, R. S.; Day, V. W. *Inorg. Chem.* **1979**, *18*, 1847–1852.

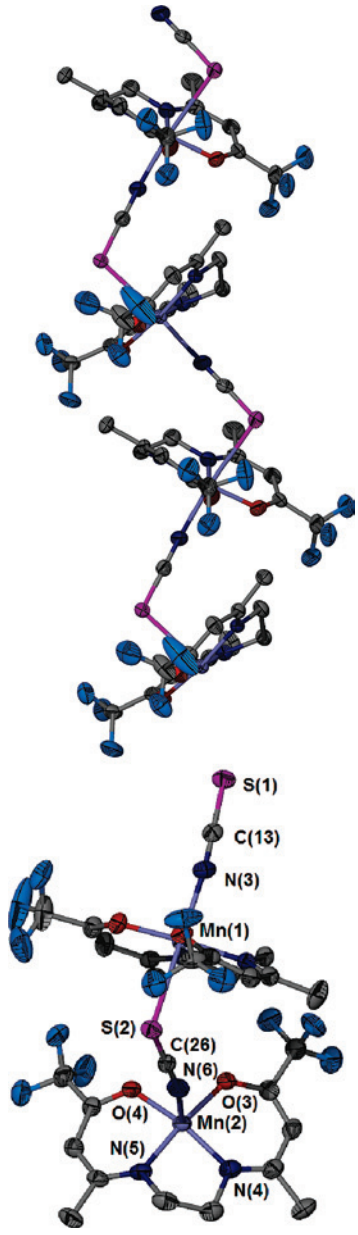

Figure 4. Thermal ellipsoid plot of complex **4** at 50% probability and the polymer chain viewed alone the *a* axis. Hydrogen atoms and CH_2Cl_2 were omitted for clarity.

indicating a nearly unhybridized sulfur anion. (See Table 3 for selected displacements and dihedral angles for complexes **2**, **3**, and **4**.)

In an attempt to isolate and crystallize a bound, ring-opened epoxide to a manganese(III) center (vita infra) complex **1** was dissolved in neat CHO and the solution left to slowly evaporate. Crystals were obtained and analyzed crystallographically, with the structure acquired being presented in Figure 5 along with pertinent bond angles and distances given in Table 2. It consists of two bridged manganese complexes where the flexible tfacacen ligand has folded back to allow for the two available coordination sites to be cis to each other. Although every attempt was made to exclude H_2O and oxygen, spurious amounts of both must have led to the oxidation of Mn(III) to Mn(IV) as no evidence of μ-hydroxo bridges was found. Boucher and Coe have synthesized two manganese(IV) salen complexes and have outlined a reaction pathway where H_2O coordinates to a manganese(III) center followed by deprotonation with a base to form a monomeric hydroxide intermediate.[29] Dimerization occurs followed by abstraction of the two hydroxo-bridging protons by a base. Oxidation and subsequent formation of the di-μ-oxo takes place in the presence of oxygen and water. A similar pathway can be envisaged, starting from a metal-bound ring-opened alkoxide protonated by water to give the azido−alcohol and the complex (tfacacen)MnOH. Dimerization of (tfacacen)MnOH follows, accompanied by the necessary deformation of the $N_2O_2^{2-}$ ligand. Proton extraction and oxidation results in the di-μ-oxo bridged species, which is seen as the thermodynamically stable product. Other di-μ-oxo manganese(IV) salen complexes have been synthesized, and all bond angles and distances for [(tfacacen)-MnO]$_2$ agree well with published data.[30,31]

Mechanistic Aspects of the Epoxide Ring-Opening Process. The reluctance of (acacen)MnX complexes to form octahedral intermediates consisting of a coordinated epoxide as an initial step in the copolymerization mechanism has been identified as a major reason manganese(III) catalytic systems have shown only modest activity for epoxide ring-opening.[12] In addition, the inability to form stable octahedral anionic intermediates with two trans coordinated apical anions should greatly inhibit copolymer propagation. Scheme 1 illustrates the various intermediates involved in the copolymerization mechanism. Initial ring-opening takes place by either a reaction first-order in the catalyst (route A) with an external initiator X^-, such as when anionic cocatalysts are employed, or by a reaction second-order in the catalyst with the initiator provided by another epoxide-bound metal species (route B).[32] In either case, an anionic octahedral complex is formed consisting of a metal alkoxide bound trans to X. A reluctance to form an octahedral complex is indicative of manganese(III) d^4 high-spin systems, where the complex is destabilized by the presence of a singly occupied e_g antibonding orbital, resulting in Jahn−Teller distortion along the z axis. For this reason, manganese(III) acacen complexes are unwilling to bind these important ligands and thus have a limited propensity toward polymer initiation and propagation.

The addition of fluorinated methyl groups to the acacen ligand was undertaken in an effort to increase the electrophilicity of the coordinatively unsaturated manganese(III) center. This in turn should increase the ability of the metal center to bind substrates such as epoxides. To understand the effect of the more withdrawing ligand, binding studies of complex **1** were undertaken in both coordinating and noncoordinating solvents (Figure 6). Essential to definitive monitoring of this process is the distinct difference seen in the asymmetric stretching frequencies of five- and six-

(29) Boucher, L. J.; Coe, C. G. *Inorg. Chem.* **1975**, *14*, 1289–1294.
(30) Torayama, H.; Nishide, T.; Asada, H.; Fujiwara, M.; Matsushita, T. *Polyhedron* **1998**, *17*, 105–118.
(31) (a) Bhaduri, S.; Tasiopoulos, A. J.; Bolcar, M. A.; Abboud, K. A.; Streib, W. E.; Christou, G. *Inorg. Chem.* **2003**, *42*, 1483–1492. (b) Ruiz-García, R.; Pardo, E.; Munoz, M. C.; Cano, J. *Inorg. Chim. Acta* **2007**, *360*, 221–232.
(32) Darensbourg, D. J.; Mackiewicz, R. M.; Phelps, A. L.; Billodeaux, D. R. *Acc. Chem. Res.* **2004**, *37*, 836–844.

Table 3. Selected Displacements and Dihedral Angles from N_2O_2 Plane for Complexes **2**, **3**, and **4**[a]

structure	Mn−N_2O_2 planar displac. (Å)	dihedral ring 1[b] to ring 2[b] (deg)	dihedral ring 1[b] to N_2O_2 plane (deg)	dihedral ring 2[b] to N_2O_2 plane (deg)
2	0.3011	10.2	5.9	−9.1
3	0.1696	31.8	−6.2	−25.9
4[Mn(1)]	0.0890	28.6	−7.8	−20.9
4[Mn(2)]	0.1278	34.5	−15.3	−19.2

[a] For a least-squares plane analysis, see the Supporting Information. [b] Ring 1 = N(1)−O(1)−C(1)−C(3), ring 2 = N(2)−O(2)−C(4)−C(6).

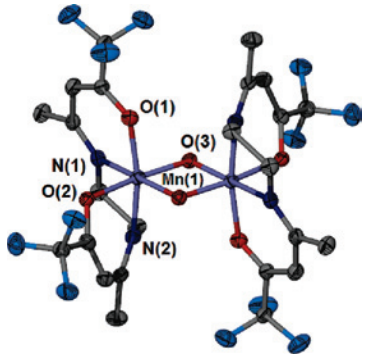

Figure 5. Thermal ellipsoid plot of [(tfacacen)MnO]$_2$ at 50% probability. Hydrogen atoms and the disordered cyclohexene oxide molecule were omitted for clarity.

Scheme 1

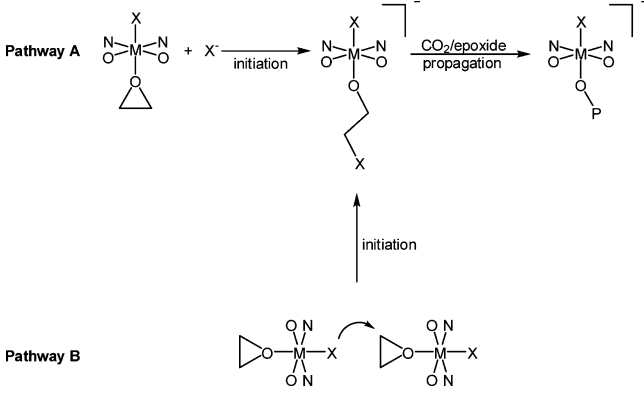

coordinate metal azides. A five-coordinate azide species is identified at 2050 cm^{-1} in CH_2Cl_2, while in coordinating CHO, a stretch representing a six-coordinate azide is apparent at 2038 cm^{-1}. A similar shift to a lower frequency of the υ_{N_3} vibration occurs with the addition of 5 equiv of strongly coordinating DMAP. With the addition of 1 equiv of (^{n}Bu)$_4$NN$_3$ in CH_2Cl_2, the formation of a diazide anionic species is apparent. The binding of CHO implies that the initial ring opening of a metal-bound, activated epoxide should be possible in the absence of an added cocatalyst (Scheme 1, route B). In addition, the ability of complex **1** to form a diazide species with only 1 equiv of azide indicates that anions in a cocatalyst/catalyst binary system may facilitate initiation and propagation of the growing polymer chain.

Complex **1** was evaluated as a catalyst for the copolymerization of CO_2 and cyclohexene oxide under typical reaction conditions (40−80 °C, 35−55 bar of CO_2 pressure, 6 h of reaction time). In cases where no cocatalyst was employed, a small amount of polymeric material was produced with turnover frequencies (TOFs) not exceeding 11 h^{-1} at 80 °C. This material was shown

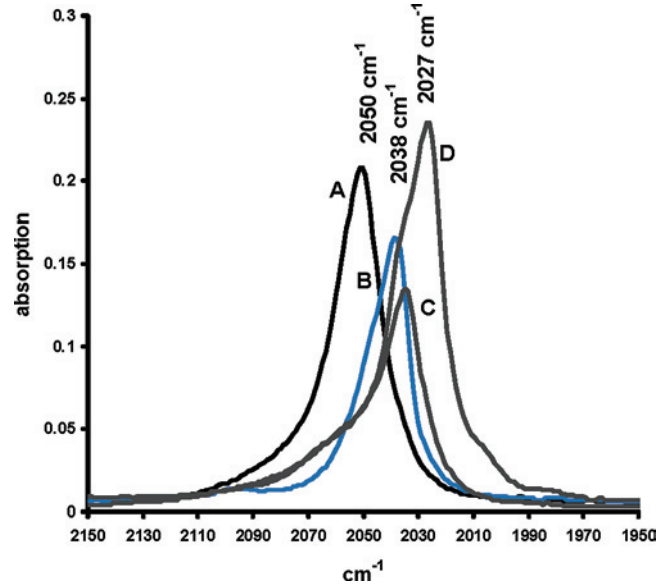

Figure 6. FTIR spectra of complex **1** in solutions of CH_2Cl_2 (A) and CHO (B). Spectra C and D are of a CH_2Cl_2 solution with 5 equiv of DMAP and 1 equiv of (^{n}Bu)$_4$NN$_3$, respectively.

to be predominately polyether with only 4−7% polycarbonate linkages. When a cocatalyst was employed, results varied widely depending on the nature of the cocatalyst. For example, with 1 or 3 equiv of DMAP, no appreciable amount of polymeric material was formed, giving only small amounts of cyclic carbonate. However, when 1 equiv of (^{n}Bu)$_4$NN$_3$ was utilized, a copolymer possessing 87% polycarbonate linkages was produced with a TOF of 2.3 h^{-1} at 80 °C. This efficiency in producing polycarbonate has parallels to chromium(III) and cobalt(III) salen systems where anionic cocatalysts not only offer high activity but are selective toward the production of polycarbonates to the exclusion of polyether and decreased amounts of cyclic carbonate formation.[33–35]

As illustrated in Scheme 1, anionic cocatalysts allow for an anion to be coordinated trans to the growing polymer chain. This activates the metal alkoxide bond (or alternately, metal carbonate) toward nucleophilic attack of the electropositive carbon of CO_2 (or epoxide) and, thus, insertion (Scheme 2). Without the use of a cocatalyst, epoxide occupies the trans coordination site, and the metal alkoxide moiety is not sufficiently nucleophilic to facilitate CO_2 insertion. Conversely, in the presence of a strong nitrogen donor,

(33) (a) Darensbourg, D. J.; Mackiewicz, R. M.; Rodgers, J. L.; Phelps, A. L. *Inorg. Chem.* **2004**, *43*, 1831–1833. (b) Darensbourg, D. J.; Bottarelli, P.; Andreatta, J. R. *Macromolecules* **2007**, *40*, 7727–7729.
(34) Cohen, C. T.; Chu, T.; Coates, G. W. *J. Am. Chem. Soc.* **2005**, *127*, 10869–10878.
(35) Lu, X. B.; Shi, L.; Wang, Y. M.; Zhang, R.; Zhang, Y. J.; Peng, X. J.; Zhang, Z. C.; Li, B. *J. Am. Chem. Soc.* **2006**, *128*, 1664–1674.

Scheme 2

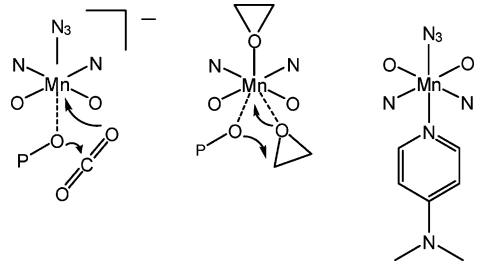

epoxide is unable to coordinate to the metal, effectively eliminating all polymer formation. Inoue reported similar phenomena when using (tpp)MnOAc for the copolymerization of CO_2 and cyclohexene oxide.[11] In that study, the addition of 1 equiv of Ph_3P, pyridine, or *N*-methylimidazole was detrimental to catalyst activity, percent carbonate linkages, and polymer molecular weight.

We can take advantage of the ability of complex **1** to bind and ring-open cyclohexene oxide to assess the mechanistic aspects of the initial ring-opening step in the copolymerization process. Referring to Scheme 1, the second-order process represented by pathway B is identical to that described by Jacobsen for the asymmetric ring-opening of cyclopentene oxide via a bimetallic reaction involving a chiral chromium(III) salen complex.[36] These researchers elucidated this bimetallic ring-opening pathway by monitoring the formation of the resulting azido alcohol by gas chromatography analysis. It would be of value to confirm the generality of this reaction course by the direct observation of the consumption of the metal azide species. Figure 7 depicts a plot of the initial rate of ring-opening versus $[\mathbf{1}]^2$, employing complex **1** at various ratios of cyclohexene oxide (CHO) in methylene chloride at 25 °C. The linear relationship observed confirms that, in this instance, in the absence of a cocatalyst, epoxide ring-opening is second-order in catalyst concentration. The greatly reduced activity of complex **1** as compared to its (salen)CrX analogs ideally facilitated this

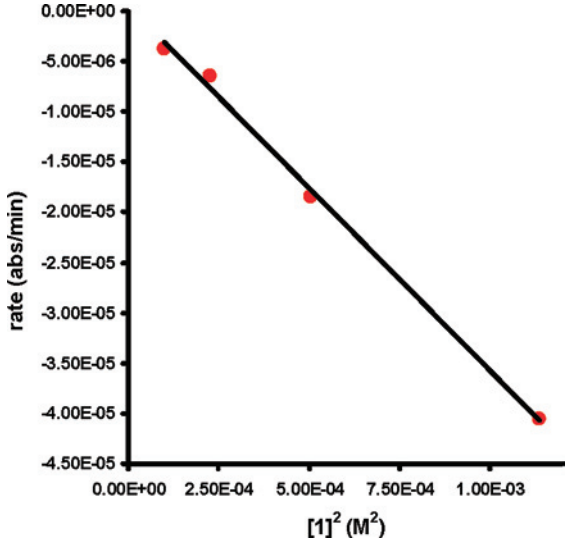

Figure 7. Linear relationship between initial rate and $[\mathbf{1}]^2$. Rates were determined by monitoring the disappearance of complex **1** at 2050 cm^{-1} by FTIR. A 2.25 M CHO solution in CH_2Cl_2 was employed with CHO/**1** ratios of 67, 100, 150, and 225.

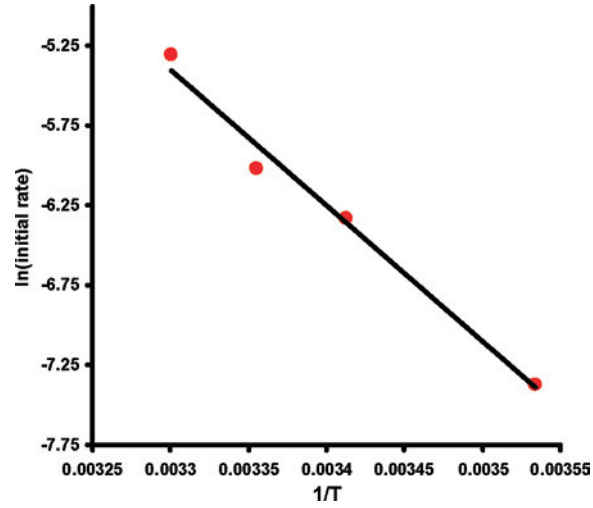

Figure 8. Arrhenius plot for the ring-opening of CHO derived from CH_2Cl_2 solutions of CHO/**1** = 67 at 10, 20, 25, and 30 °C.

study.[37] The activation energy for this second-order process was determined from an Arrhenius plot of the ln(initial rate) versus temperature and was found to be 71.0 ± 6.0 kJ/mol (Figure 8).

With the bimetallic process confirmed, a study of the monometallic ring-opening of an epoxide assisted by a cocatalyst (pathway A) was undertaken. The reaction of complex **1** with 150 equiv of CHO and 1 equiv of DMAP in CH_2Cl_2 at 40 °C was monitored by FTIR. In stark contrast to the cleanly defined absorptions in the υ_{N_3} region observed in the bimetallic process, a number of overlapping azide stretching frequencies ranging from 2040 to 2095 cm^{-1} rapidly developed, thus prohibiting detailed rate analysis (Figure 9). In addition, the formation of organic azide was retarded as evidenced by the more than 4 h required to completely consume the metal azide stretch at 2040 cm^{-1} (when compared to 1.5 h in the absence of DMAP). Statistical deconvolution revealed four bands midway through the reaction at 2042, 2062, 2073, and 2093 cm^{-1}. The bands at 2042 and 2093 cm^{-1} can be assigned to the six-coordinated manganese azide and organic azide, respectively. The remaining two bands at 2062 and 2073 cm^{-1} are ostensibly attributed to metal azides of alternate coordination number or bonding mode. A large amount of literature exists concerning metal−azide binding and coordination with salen-type Schiff-base ligands and di-, tri-, and tetradentate nitrogen-containing ligands of manganese(III),[24] manganese(II),[38] and cobalt(III).[39] Definitive descriptions regarding the nature of these species is not possible on the basis of infrared data alone. However, considering the flexibility of the tfacacen

(36) (a) Martinez, L. E.; Leighton, J. L.; Carste, D. H.; Jacobsen, E. N. *J. Am. Chem. Soc.* **1995**, *117*, 5897–5898. (b) Hansen, K. B.; Leighton, J. L.; Jacobsen, E. N. *J. Am. Chem. Soc.* **1996**, *118*, 10924–10925.
(37) (a) Darensbourg, D. J.; Yarbrough, J. C. *J. Am. Chem. Soc.* **2002**, *124*, 6335–6342. (b) Darensbourg, D. J.; Mackiewicz, R. M.; Rodgers, J. L.; Fang, C. C.; Billodeaux, D. R.; Reibenspies, J. H. *Inorg. Chem.* **2004**, *43*, 6024–6034.

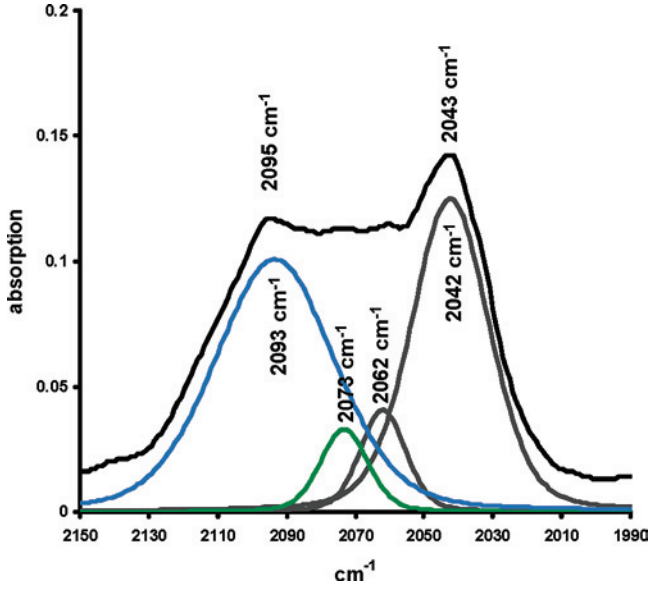

Figure 9. FTIR spectrum of a reaction at 40 °C of CHO/**1** = 150 in CH_2Cl_2 with 1 equiv of DMAP at 73 min. The underlying curves represent a statistical deconvolution of asymmetric azide stretches.

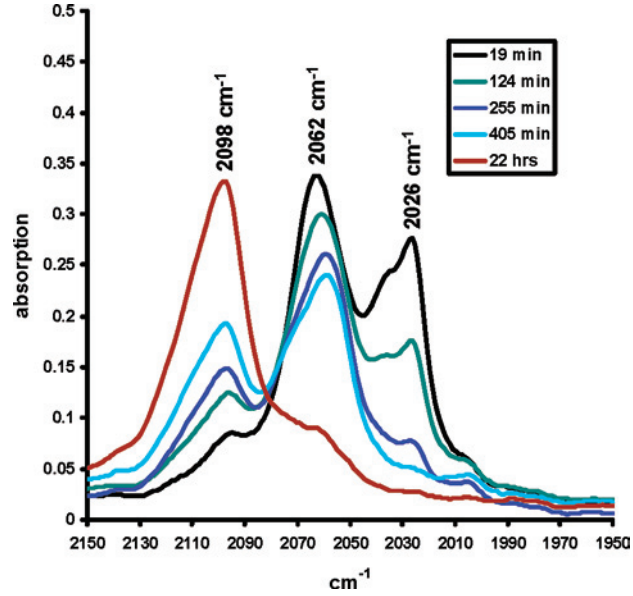

Figure 10. FTIR spectra of a reaction of CHO/**1** = 100 in CH_2Cl_2 with 1 equiv of $(^nBu)_4NN_3$ at 40 °C.

ligand, numerous possibilities exist including cis bound terminal azide/azide or azide/donor ligands, bridged $\mu_{1,1}$/$\mu_{1,3}$ (EO or EE) bimetallic azides complexes, or 1-D azide coordination polymers.

Similar behavior was observed upon the addition of 1 equiv of $(^nBu)_4NN_3$ to a CH_2Cl_2 solution of complex **1** with a CHO/**1** ratio of 100 at 40 °C (Figure 10). The anticipated diazide species is observed at 2026 cm^{-1}; however, there is rapid formation of an intense peak at 2062 cm^{-1}. Within 4 h, the diazide species is consumed, leaving the absorbance at 2062 cm^{-1} and organic azide at 2098 cm^{-1}. Full conversion to organic azide is not achieved until more than 20 h into the reaction. This is approximately 9 times slower than the bimetallic reaction involving complex **1** at the same CHO/**1** ratio.

Without structural information as to the identity of the new metal azide species in the presence of Lewis bases, the underlying reason for the decreased reaction rate is unclear. The formation of the species at 2062 cm^{-1} is reproducible in the absence of epoxide, and its formation is enhanced by heat. Thus, the more thermodynamically stable species may be unable to readily bind epoxide via displacement of the

Scheme 3

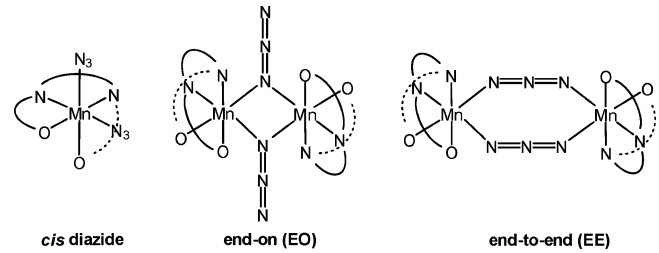

anions of a diazide species. If the tfacacen ligand were to adopt a nonplanar bonding mode, the two available coordination sites would be either cis in a monometallic diazide complex or occupied by bridging azides (Scheme 3). In the former case, the requisite activation of a bound epoxide or anion as facilitated by a trans donor ligand, and thus subsequent activation toward ring-opening, would be very low. The latter case seems less likely as it would require the loss of an azide, resulting in the formation of "free azide" anion, a species which formed in only small quantities throughout the reaction. In any case, this behavior is not a likely model for the chromium and cobalt salen catalytic systems due to its slow rate of ring-opening and susceptibility to alternate bonding modes.

Considering the critical features the azide moiety provides to the mechanistic study of the copolymerization of CO_2 and epoxides, it would be advantageous if other highly active anions possessing such convenient infrared stretching frequencies could be utilized. Azide falls into the larger category termed the pseudohalogens of which the most important are cyanide (CN^-), cyanate (OCN^-), and thiocyanate (SCN^-).[40] Boucher and Day have prepared several manganese(III) acacen complexes with these anions and reported stretching frequencies indicative of a *N*-bound anions.[23] For first-row

(38) (a) Liu, C.-M.; Gao, S.; Zhang, D.-Q.; Liu, Z.-L.; Zhu, D.-B. *Inorg. Chim. Acta* **2005**, *358*, 834–838. (b) Ghosh, A. K.; Ghoshal, D.; Zangrando, E.; Ribas, J.; Chaudhuri, N. R. *Inorg. Chem.* **2005**, *44*, 1786–1793. (c) Ni, Z.-L.; Kou, H.-Z.; Zheng, L.; Zhao, Y.-H.; Zhang, L.-F.; Wang, R.-W.; Cui, A.-L.; Sato, O. *Inorg. Chem.* **2005**, *44*, 4728–4736. (d) Bai, S.-Q.; Gao, E.-Q.; He, Z.; Fang, C.-J.; Yue, Y.-F.; Yan, C.-H. *Eur. J. Inorg. Chem.* **2006**, 407–415. (e) Yu, M.-M.; Ni, Z.-H.; Zhao, C.-C.; Cui, A.-L.; Kou, H.-Z. *Eur. J. Inorg. Chem.* **2007**, 5670–5676.

(39) (a) Massoud, S. S. *Polyhedron* **1994**, *13*, 3127–3134. (b) Goher, M. A. S.; Al-Salem, N. A.; Mautner, F. A. *Polyhedron* **1997**, *21*, 3747–3755. (c) Massoud, S. S.; Mautner, F. A.; Abu-Youssef, M.; Shuaib, N. M. *Polyhedron* **1999**, *18*, 2287–2291. (d) Sharma, R. P.; Sharma, R.; Bala, R.; Quiros, M.; Salas, J. M. *J. Coord. Chem.* **2003**, *56*, 1581–1586. (e) Sharma, R. P.; Sharma, R.; Bala, R.; Singh, K. N.; Pretto, L.; Ferretti, V. *J. Mol. Struct.* **2006**, *784*, 109–116. (f) Sharma, R. P.; Sharma, R.; Bala, R.; Venugopalan, P. *J. Mol. Struct.* **2006**, *787*, 69–75. (g) Sharma, R. P.; Sharma, R.; Bala, R.; Burrows, A. D.; Mahon, M. F.; Cassar, K. *J. Mol. Struct.* **2006**, *794*, 173–180.

(40) Nakamoto, K. *Infrared and Raman Spectra of Inorganic and Coordination Compounds*, 5th ed.; Wiley & Sons, Inc.; New York, 1997; Section III-16, Part B, pp 116−126.

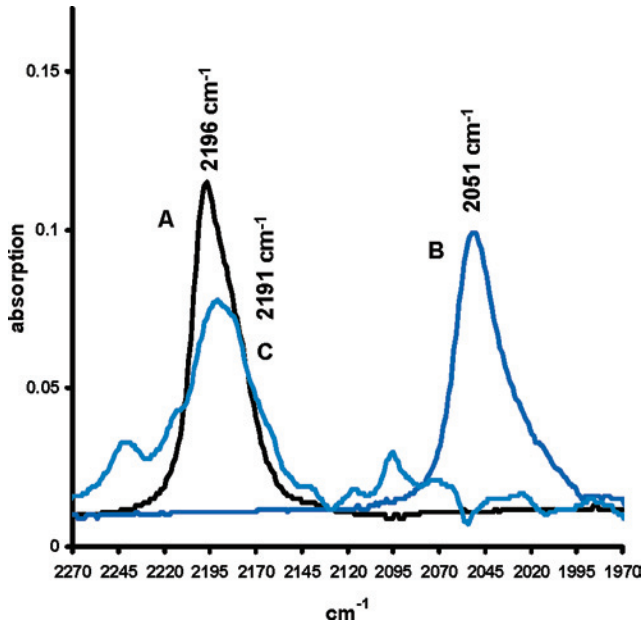

Figure 11. FTIR spectra of CH_2Cl_2 solutions of (**A**) complex **3**, (**B**) complex **4**, and (**C**) a reaction mixture following the ring-opening of CHO by complex **4**.

transition metals, *N*-bonded isothiocyanates predominate and display an asymmetric stretch from 2050 to 2080 cm^{-1} if terminally bound and in the vicinity of 2100 cm^{-1} or higher if bridged end-on (through nitrogen) or end-to-end.[26,41,42] Cyanates also show a strong preference for binding through nitrogen, thus giving isocyanate complexes with stretching frequencies ranging from 2100 to 2300 cm^{-1} for typical binding modes.[40,43]

Complexes **3** and **4**were prepared and evaluated for their ability to ring-open cyclohexene oxide in the same manner as described with complex **1**. Figure 11 displays the infrared stretching frequencies of five-coordinate manganese(III) isocyanate and isothiocyanate in CH_2Cl_2. For complex **3**, a stretching band containing a slight shoulder is evident at 2196 cm^{-1} and is typical of isocyanate complexes. For complex **4**, a stretch similar in appearance to that of **3** is seen at 2051 cm^{-1} and is typical for a nitrogen-bound isothiocyanate complex. Presumably, the ring-opening of cyclohexene oxide by a thiocyanate anion proceeds along a bimetallic pathway where a metal-bound isothiocyanate nucleophilicity attacks the α carbon of a coordinated epoxide though the carbon−sulfide moiety. This in turn would lead to a ring-opened metal-bound alkyl thiocyanate alkoxide. A reaction carried out with a CHO/**4** ratio of 67 at 40 °C in CH_2Cl_2 for 2 h was monitored by FTIR and resulted in the complete consumption of metal-bound isothiocyanate and the formation of a broad stretch at 2191 cm^{-1} (Figure 11). This latter species is in good agreement with alkyl−thiocyanates synthesized by other methods.[44] Interestingly, organic thiocyanates have been produced through the ring-opening of epoxides with ammonium thiocyanate in the presence of TPP transition metal complexes, tetraarylporphrin derivatives, and aza-crown ethers.[45] This, combined with the fact that the ring-opening of CHO with **4** proceeds at rates comparable to those with **1** under similar reaction conditions, indicates that the thiocyanate anion may be well-suited as an initiator for the copolymerization of CO_2 and epoxides.

The effectiveness of cyanate is less clear, though preliminary results show that **3** catalyzes the ring-opening of CHO at a considerably lower rate. In a reaction with a CHO/**3** ratio of 100:1 at 40 °C in CH_2Cl_2, no appreciable amount of organic product was observed by FTIR until more than 20 h of reaction time had passed. Eventually, a product does appear at 2261 cm^{-1} and is ostensibly assigned to that of organic cyanate in analogy to the production of organic thiocyanate from an isothiocyanate initiator. However, alkyl cyanates are rare, whereas alkyl isocyanates are well-known organic compounds.[46] Indeed, organic isocyanates show absorbances in the range of 2200−2300 cm^{-1}, though the formation of such a product seems contrary to the nucleophillic attack of the carbonyl moiety of a nitrogen-bound isocyanate.

Conclusions

The synthesis and structural characterization of Schiff base complexes of the formula (tfacacen)MnX (X = Cl, N_3, NCO, NCS) have been described. The presence of the highly electron-withdrawing $-CF_3$ substituents in these derivatives, as compared to their acacen analogs, has enabled these d^4 high-spin complexes to readily bind to a sixth ligand, for example, epoxides. This property has made it possible to monitor the epoxide ring-opening pathway utilizing the υ_{N_3} vibrational mode in (tfacacen-)MnN_3. In this instance, the ring-opening reaction was demonstrated to be second-order in metal complex, analogous to the well-studied (salen)CrX system. Relative to the chromium(III) salen derivatives, the (tfacacen)MnX derivatives are considerably slower at facilitating the epoxide ring-opening process. Concomitantly, because of the electrophilicity of the manganese(III) complexes, their effectiveness at promoting the CO_2 insertion process is greatly reduced compared to the (salen)CrX and (salen) CoX derivatives. Hence, the manganese(III) complexes are not efficient catalysts for the copolymerization of

(41) Boudalis, A. K.; Clemente-Juan, J.-M.; Dahan, F.; Tuchagues, J.-P. *Inorg. Chem.* **2004**, *43*, 1574–1586.

(42) Mauro, A. E.; Haddad, P. S.; Zorel, H. E., Jr.; Santos, R. H. A.; Ananias, S. R.; Martins, F. R.; Tarrasqui, L. H. R. *Trans. Met. Chem.* **2004**, *29*, 893–899.

(43) Youngme, S.; Phatchimkun, J.; Suksangpanya, U.; Pakawatchai, C.; van Albada, G. A.; Reedijk, J. *Inorg. Chem. Commun.* **2005**, *8*, 882–885.

(44) (a) Fujiki, K.; Yoshida, E. *Synth. Commun.* **1999**, *29*, 3289–3294. (b) Renard, P.-Y.; Schwebel, H.; Vayron, P.; Leclerc, E.; Dias, S.; Mioskowski, C. *Tetrahedron Lett.* **2001**, *42*, 8479–8481. (c) Iranpoor, N.; Firouzabadi, H.; Nowrouzi, N. *Tetrahedron* **2006**, *62*, 5498–5501.

(45) (a) Sharghi, H.; Nasseri, M. A.; Nejad, A. H. *J. Mol. Catal.* **2003**, *206*, 53–57. (b) Sharghi, H.; Nejad, A. H.; Nasseri, M. A. *New J. Chem.* **2004**, *28*, 946–951. (c) Sharghi, H.; Beni, A. S.; Khalifeh, R. *Helv. Chim. Acta* **2007**, *90*, 1373–1385.

(46) March, J.; Smith, M. S. *March's Advanced Organic Chemistry: Reactions, Mechanisms, and Structure*, 5th ed.; Wiley & Sons, Inc.; New York, 2001.

epoxides and CO_2 to afford polycarbonates. Unlike the greatly enhanced reactivity of the (salen) CrX and (salen)CoX complexes toward CO_2/epoxide coupling in the presence of Lewis base cocatalysts (e.g., anions and *N*-heterocyclic amines), (tfacacen)MnX complexes were shown to be greatly inhibited in relation to this process upon the addition of such cocatalysts. Current studies in our laboratory are directed at assessing the binding abilities of ligands such as epoxides and *N*-heterocyclic amines to (salen)MnX complexes for comparison with the herein reported (tfacacen)MnX derivatives.

Acknowledgment. We gratefully acknowledge the financial support from the National Science Foundation (CHE-0543133) and the Robert A. Welch Foundation (A-0923).

Supporting Information Available: X-ray crystallographic files in CIF format for the structure determinations of complexes **2**, **3**, **4**, and $[(tfacacen)MnO]_2$ and a table giving the least-squares plane analysis for crystal structures. The material is available free of charge via the Internet at http://pubs.acs.org.

IC800286P